One step dual template facile synthesis of Micro-Mesoporous ZSM-5 Composite and its application in 5-(ethoxymethyl)furfural (biofuel additive) synthesis

Prajakta N. Manal
CSIR-National Chemical Laboratory
Prashant S. Niphadkar
CSIR-National Chemical Laboratory
Sachin U. Nandanwar
CSIR-National Chemical Laboratory
Vijay V. Bokade (vv.bokade@ncl.res.in)
CSIR-National Chemical Laboratory

Research Article

Keywords: ZSM-5, Micro-Meso composite, Fructose, Ethoxymethyl furfural- biofuel additive

Posted Date: June 22nd, 2022

DOI: https://doi.org/10.21203/rs.3.rs-1737411/v1

Abstract

The preparation of micro-mesoporous zeolite with controlled mesoporosity is an expanding area of research having advantages in term of the creation of mesoporosity by preserving crystallinity of zeolite; converting bulky molecules to valuable products etc. The present work is a successful attempt to synthesize micro-meso ZSM-5 composite in one step using cheaper silica (sodium silicate) and alumina (aluminiumsulphate) as source material with dual templates (CTMABr and TPABr). The insitu mesoporous creation in a controlled way by using these source materials is rarely reported. The facile one-step synthesis of micro-mesoporous ZSM-5 composite feature dual Meso/microporosity by the marginal decrease in crystallinity(71%)and mesoporous creation in micro-ZSM-5 found to be depend on optimum CTMABr/SiO_2 molar ratio in the range of 0.04 to 0.06. The micro-mesoporous ZSM-5 composite zeolite was evaluated for cascade synthesis of 5-EMF (ethoxymethyl furfural- biofuel additive) from fructose, exhibited 5 fold increase in EMF yield of 24.2% than micropous ZSM-5 4.6%.

1. Introduction

ZSM-5 is an industrially important zeolite having wide applications in the area of petroleum and petrochemical industries. The unique straight and zigzag channel structure, hydrothermally stable and catalytically acidic site makes ZSM-5 attractive catalyst for many reactions such as cracking,[1, 2] alkylation,[3, 4] acylation,[5] isomerization,[6] aromatization,[7] and aldol condensation etc.[8–10] However, ZSM-5 have limitations to catalyze bulky reagent due to small micro pore size (0.55nm) which impose diffusional constraints in the micropore channels.[11]

Significant research efforts have been made in the past two decade to prepare micro-mesoporous composite zeolites, by insitu dual templates well as post modifications methods such as dealumination and desilication.[11–16] Amongst these methods, generation of mesoporosity by in situ method has certain advantages over post modification methods in terms of simple synthesis, avoid multi steps to follow which also account towards increase in cost. Thus, this work is an attempt to create mesoporosity in ZSM-5 by in situ dual template method. Goncalves et al.[15] reported synthesis of mesoporous ZSM-5 by aging initial gel mixture at 30–90□C for 18–72 h followed by addition of cetyltrimethyl ammonium cation (CTABr) and crystallization at 120–150□C, achieved dual phase of MCM-41 and ZSM-5. However mesoporous ZSM-5 prepared by this method shows higher contribution of amorphous material due to formation of MCM-41 than crystalline microporous ZSM-5. Quanyiwang et al.[14] reported mesoporous ZSM-5 using single step hydrothermal method using two mesoporous templates such as dimethyl octadecyl[3-(trimethoxysilyl)propyl] ammonium chloride (TPOAC) and CTABr, leads to formation mesoporous ZSM-5, but with very low crystallinity. Hierarchical lamellar mesoporous ZSM-5 reported by Laleh Emdadi et al.[11], was synthesized by using diquaternary ammonium surfactant ($[C_{22}H_{45}\text{-}N^{+}(CH_3)_2\text{-}C_6H_{12}\text{-}N^{+}(CH_3)_2\text{-}C_6H_{13}]Br^{-}{}_2$) templateat 150□C. In the prior art, mesoporous ZSM-5 was synthesized by dual template insitu method has comparatively higher mesopore volume and mesopore surface area assigned as external surface area than micropore volume and surface area. This mesoporosity

generation in excess has destroyed the ZSM-5 framework in a major way and increases the contribution of amorphous nature which limits its application as micro-meso composites. Presence of micropores in ZSM-5 is also required for many applications to have shape selective nature, which is primary advantage. Thus, proper combination of Micro-Meso porosity in ZSM-5 in control manner by minimizing destruction of ZSM-5 framework is necessary. Another important parameter in synthesis of micro-mesoporous ZSM-5 is use of raw material. It is always recommended to use easily available and cheap source of silica and alumina to make Micro-mesoZSM-5 composite cost effective. As per the reported information, comparatively expensive raw material such as tetra ethyl orthosilicate, aluminiumisoproxide, tetrapropyl ammonium hydroxide[11, 14–16] were used at higher crystallization temperature and time. Here, we report probably the synthesis of micro-mesoporous ZSM-5 composite with controlled mesoporous generation using cheaper silica and alumina source at conventional hydrothermal treatment.

. The facile one step synthesis of micro-mesoporous ZSM-5 composite was carried out using cheaper sodium silicate, aluminium sulphate with dual templates: tetra propyl ammonium bromide (structure directing agent) along with CTABr act as meosporous template in one step hydrothermal treatment. These synthesized micro-meso ZSM-5 composites were further evaluated for fructose to 5-EMF reaction.

2. Experimental

2.1. Preparation of micro-mesoporous ZSM-5 composite

Micro-mesoporousZSM-5 composites were prepared by one step hydrothermal crystallization process using molar gel composition: SiO_2/0.01Al_2O_3/0.3Na_2O/0.1 TPABr/xCTMBr/36 H_2O,where X = 0.04, 0.06 and 0.1. Typically, 7.86g of TPABr (98%, Loba chemie) and 30.0g DI water was dissolved under stirring to make Solution A. Separately, Solution B was prepared, by mixing of 62.60g of sodium silicate (28% SiO2 & 8% Na2O, Loba chemie)in 30.0g of water under vigorous stirring. Then, solution B was slowly added to solution A and named as solution C. 1.92g of Aluminium sulphate(99%, Loba chemie) was carefully dissolved in acidic solution containing 5.13g of Sulphuric acid (98%, Loba Chemie) and 10.0g water, this alumina solution (solution D) was then slowly added to solution C under vigorous stirring for 2h, designated as solution E. Finally 6.3g of Cetyltrimethyl ammonia bromide (CTMABr, 98%, Loba Chemie) dissolved in 69.5g of water was added in solution E under stirring for 1h to make final gel. Final gel was then transferred into SS autoclave and subjected to the hydrothermal crystallization at 160°C for 48 h. After hydrothermal crystallization, gel was separated into wet cake by vacuumed filtration, then dried at 120°C and calcined in muffle furnace at 550^oC for 10h to have micro-meso ZSM-5 composite in Na-form. The ammonium form of this composite was obtained by three consecutive exchanges with 10 ml 1M NH_4Cl solution per g at 80°C for 3h., followed by drying and calcination at 500°C for 5hr to convert NH4 form of composite to H form. The final sample is designated as ZSM-$5_{CTA-0.06}$, similarly other samples were prepared with CTMABr/SiO_2 = 0.04 and 0.1 were designated as ZSM-$5_{CTA-0.04}$ and ZSM-$5_{CTA-0.1}$.

2.2. Catalyst Characterization:

Different characterization techniques were opted to study the synthesized catalysts. The catalyst were characterized by Powder X-ray diffraction (XRD) (Cu Kα) in the low and wide angle range of 2–15 and 5–50□2Θ, respectively on RigakuMultiflex 600 powder diffractometer with a scan rate of 5 deg per minute. Nitrogen sorption isotherms were obtained using Micromeritics ASAP 2010 instrument. During analysis 0.5gm of each sample was treated and specific surface area was estimated by the BET equation, while the pore size distribution and the mesopore analysis were determined from the desorption as well as from adsorption branch of nitrogen isotherms using Barette-Joyner-Halenda (BJH) method. Micropore volume was estimated by the t-plot analysis using adsorption branch of isotherms. Transmission electron Microscopy (TEM) were obtained using TECNAI instrument with a resolution power of 2nm. Scanning Electron microscopy (SEM) data for morphological identification were obtained using FEI Nova Nano SEM 450 employed with field emission gun in different nanometer range for better catalytic study.

2.3. Catalytic performance

Fructose to 5-EMF reaction over micro- ZSM-5, Micro-meso composites: ZSM-$5_{CTA-0.04}$,ZSM-$5_{CTA-0.06}$ and ZSM-$5_{CTA-0.1}$were carried out in a 30 ml stainless steel pressure autoclave. The temperature was maintained with an accuracy of ± 0.5 K by a PID controller. In typical reaction, 0.57 g Fructose (99% ,Merck)- and 0.3 g (50% with respect to substrate-Fructose) catalyst and 15 ml ethanol (99% ,Merck)was placed in autoclave. The reaction was performed in the temperature range of 120-175^{o}C for 8h at 600 rpm. After the reaction, autoclave was allowed to cool naturally and was analyzed on HPLC.

The yield of 5-HMF (hydroxymethyl furfural) and 5-EMF were analysed on Agilent 1260 Infinty HPLC installed with UV detector and RI detector. The separation of HMF and EMF was obtained using Hiplex H (300 X 7.7mm) HPLC column. A detection wavelength of 280 nm was fixed to distinguish separation of product. Also the conversion of sugars were obtained on RI detector (35^{o}C). The single mobile phase 0.005M Sulphuric acid with a flow rate of 0.6 ml/min was selected for the separation of product as well as sugars. Yield was calculated from calibration curve.

Yield was calculated as:

Yield of EMF (%) = [(moles of EMF produced) / (initial moles of fructose)] × 100

Yield of HMF (%) = [(moles of HMF produced) / (initial moles of fructose)] × 100

3. Results And Discussion

3.1 Textural and Morphological properties of Micro-Mesoporus ZSM-5 Composite

Effect of CTMABr as template for creation of mesoporosity was studied by varying CTMABr/SiO_2 molar ratio, keeping other composition constant. Fig. S-1 and Fig. 1 represents the powder XRD patterns of ZSM-5, ZSM-$5_{CTA-0.04}$, ZSM-$5_{CTA-0.06}$ and ZSM-$5_{CTA-0.1}$ in as synthesized and H-form, respectively. As

shown in Fig S-1, The low angle XRD pattern of as synthesized micro-meso ZSM-5 composite showed only one peak at 2θ° = 2.6 with low intensity, which confirmed generation of mesopores in ZSM-5 [15, 16]. However, the low angle diffraction peaks disappeared upon calcination which is required to remove organic templates (Fig. 1), similar observation is reported by Wang et al[14] with CTMABr and Dimethyl octadecyle as dual template. Wide angle XRD pattern (Fig. 1) of ZSM-5, ZSM-$5_{CTA-0.04}$, ZSM-$5_{CTA-0.06}$ and ZSM-$5_{CTA-0.1}$ exhibits wide-range structural ordering characteristic of MFI type zeolite. As can be seen, no other unidentified/mixed phases were observed, indicated that synthesized samples are having pure MFI phase. Upon addition of CTMABr, the relative crystallinity of micro-ZSM-5 and micro-meso ZSM-5 is quite different. The conventional micro- ZSM-5 has the highest relative crystallinity than micro-mesoZSM-$5_{CTA-0.04}$ (82%), ZSM-$5_{CTA-0.06}$ (71%) and ZSM-$5_{CTA-0.1}$(80%). This is mainly due to small framework thickness of micro-meso ZSM-5 along the *b*-axis direction compared to three-dimensional microporous ZSM-5 zeolite.[17]

The surface area, pore size and pore volume for all synthesized samples are determined by Low temperature (−196^{o}C) nitrogen adsorption-desorption analysis, Fig. 2 depict isotherms for ZSM-5, ZSM-$5_{CTA-0.04}$, ZSM-$5_{CTA-0.06}$, and ZSM-$5_{CTA-.0.1}$ samples. The conventional ZSM-5 exhibits type I isotherm (IUPAC classification) depicting high uptake at low relative pressures, which is a characteristics of microporous zeolitic structures without mesoposity. This is also confirmed by pore size distribution curve in Fig. S-2, shows a hysteresis loop associated with presence of interparticle voids.[17]

In case of micro-meso ZSM-$5_{CTA-0.04}$, ZSM-$5_{CTA-0.06}$, and ZSM-$5_{CTA-.0.1}$ display combination of both type I and type IV isotherms[18], indicates the existence of both microporous and mesoporous pores. At low relative pressure (P/P0 < 0.45), isothermsforZSM-$5_{CTA-0.04}$, ZSM-$5_{CTA-0.06}$, and ZSM-$5_{CTA-.0.1}$ is identical as that of micro-ZSM-5. At higher relative pressure (P/P0 > 0.45), a hysteresis loops appeared in the isotherms of ZSM-$5_{CTA-0.04}$,ZSM-$5_{CTA-0.06}$, and ZSM-$5_{CTA-.0.1}$. Hysteresis loops of ZSM-$5_{CTA-0.06}$ isotherm is wide, while in case of ZSM-$5_{CTA-0.04}$ and ZSM-$5_{CTA-.0.1}$, a hysteresis loops are relatively narrow, and uneven in pattern. This indicates that ZSM-$5_{CTA-0.04}$ and ZSM-$5_{CTA-.0.1}$ have disordered mesopores and broad pore size distribution. In case of ZSM-$5_{CTA-0.06}$, mesopores is also disorder but pore size distribution is comparatively uniform.[19]

Fig S2 shows the pore size distribution of ZSM-$5_{CTA-0.04}$, ZSM-$5_{CTA-0.06}$, and ZSM-$5_{CTA-.0.1}$. The mesopore size of ZSM-$5_{CTA-0.04}$ andZSM-$5_{CTA-.0.1}$ centered around 2.5 nm, in addition this, ZSM-$5_{CTA-0.04}$ have broad mesopore size distribution in 3 to 4nm. In case of ZSM-$5_{CTA-0.06,}$ pore size is centered around 3 nm and relatively higher intensity indicates a higher and uniform mesopore formation in ZSM-$5_{CTA-0.06}$ than ZSM-$5_{CTA-0.04}$ andZSM-$5_{CTA-.0.1}$. As suggested from the shape of hysteresis loops in their isotherms their mesoporous and pore size distribution, meoporous zeolite has mesopore size distribution in the range 2,5 to 3 nm. In contrast, conventional ZSm-5 does not have significant mesoporosity.

Textural property of ZSM-5,ZSM-$5_{CTA-0.04}$, ZSM-$5_{CTA-0.06}$, and ZSM-$5_{CTA-.0.1}$ sample are tabulated in Table-1. It show that the sample ZSM-$5_{CTA-0.04}$, ZSM-$5_{CTA-0.06}$ possess higher external/mesoporous surface area of 72 and 98 m^2/g respectively and mesopore volume of 0.09 and 0.10 cc/g, respectively than micro-ZSM-5 (30 m^2/g and 0.05 cc/g). The micropore surface area (340 and 323 m^2/g) and micropore volume (0.15 & 0.14 cc/g) of ZSM-$5_{CTA-0.04}$, ZSM-$5_{CTA-0.06}$ respectively are lower than that of micro-ZSM-5 (372 m_2/g and 0.16 cc/g). Higher external/mesoporous surface area and mesopore volume of ZSM-$5_{CTA-0.04}$ and ZSM-$5_{CTA-0.06}$ confirmed the formation mesoporous without destroying the microporous ZSM-5 framework structure. ZSM-$5_{CTA-.0.1}$ also possess higher mesopore surface area of 63m^2/g and meso-volume of 0.08 cc/g than ZSM-5 however it is lower than ZSM-$5_{CTA-0.04}$ and ZSM-$5_{CTA-0.06}$.

Scanning electron microscopy was employed to provide detailed insights into the morphological changes of synthesized micro-meso ZSM-5 composite. Figure 3 represent SEM image of micro-ZSM-5, micro-mesoZSM-$5_{CTA-0.04}$, and micro-mesoZSM-$5_{CTA-0.06}$. Particle of conventional micro- ZSM-5 is spherical in shape with 1 to 4µm size whereas ZSM-$5_{CTA-0.04}$and ZSM-$5_{CTA-0.06}$ hows lamellar MFI structure formed as plate like structure stacked into porous spherical aggregate (inset of Fig. 3b & c). Furthermore the surface of ZSM-$5_{CTA-0.04}$,and ZSM-$5_{CTA-0.06}$ are rough and porous whereas the surface of the conventional micro-ZSM-5 is smooth and porous structure. Laleh Emadadi and Quanyi Wang et. al [11, 15] reported similar type of morphology for mesoporous ZSM-5 synthesized using Diquaternary ammonium surfactant and combination of CTAB and TPOAC as template, respectively.

In order to observe clear morphologies and to confirm mesoporosity, TEM analysis was also performed. Figure 4 depict TEM image of micro-ZSM-5 &optimum micro-meso ZSM-$5_{CTA-0.06}$. Figure 4(a) shows fully packed fusion of crystals in compliance with data obtained from SEM. The fusion of crystal arrangement in ZSM-5 is thick with bulky accordance, while in the TEM image of ZSM-$5_{CTA-0.06}$ (Fig. 4b), spherical shaped transparency within fused crystal clearly indicates the formation of mesoporous structure whereas it is absent in conventional micro-ZSM-5. This specify that the organic moieties (Anionic surfactant template) could accomplish a better interaction rather than inorganic silicates. Also the magnified TEM image of ZSM-$5_{CTA-0.06}$ (Fig. 4c and d)shows a uniform distribution of mesoporous structure. The lattice finges obtained in TEM image of ZSM-$5_{CTA-0.06}$ explains the presence of micro and mesopores within the ZSM-$5_{CTA-0.06}$ catalyst.

^{29}Si MAS NMR and ^{27}Al MAS NMR were performed to investigate the local coordination environments of silicon and aluminum. Figure 5 (a) represents the ^{29}Si NMR of micro-ZSM-5, micro-meso ZSM-$5_{CTA-0.04}$,and ZSM-$5_{CTA-0.06}$. The spectrum of ZSM-5 shows three resonance peak at -107, -113. and − 117 ppm which were assigned to Si(0Al) (Q^4), 3Si(1Al) and crystallographic in equivalent sites of Si(0Al) (Q^4) sites, respectively[15, 20]. While spectra of ZSM-$5_{CTA-0.04}$,and ZSM-$5_{CTA-0.06}$ display four resonance peak at -107, -113. -117 and − 100 ppm. Additional peak at-100 ppm may be assigned to silanol group ($(SiO)_3SiOH$, Q^3).[20]. However, peak at -100 ppm is absent in conventional micro-ZSM-5. Appearance of

silionol group possibly come from mesoporous surface in ZSM-$5_{CTA-0.04}$, ZSM-$5_{CTA-0.06}$, and ZSM-$5_{CTA-.0.1}$[15].

Figure 5 (b) represents ^{27}Al NMR of micro-ZSM-5, micro-mesoZSM-$5_{CTA-0.04}$, and micro-mesoZSM-$5_{CTA-0.06}$. Single resonance peak at ~ 55 ppm assigned to tetrahedral coordinated Al is seen in conventional micro-ZSM-5. On other hand, ZSM-$5_{CTA-0.04}$, and ZSM-$5_{CTA-0.06}$ shows two peak centered at ~ 55 ppm and 0 ppm. Peak at 0 ppm is ascribed to the octahedral aluminum, associated with the non framework aluminum species[18]. The generation of mesoporous in ZSM-5 gives signal at 0ppm, which is corresponding decrease in crystallinity of ZSM-5 matches well with XRD patterns.

3.2 Proposed Micro-Mesopore ZSM-5 Composite mechanism

A schematic illustration for formation of micro-mesoporous ZSM-5 composite is shown in Scheme 1. Initially, zeolite precursors (Si, Al, TPA) along with surfactant (CTA) are mixed at room temperature. In general, the formation of mesophases (M41S) during nucleation and crystallization is not fafavourable path 1) due to specific molar gel composition and hydrothermal crystallization conditions. However, XRD studies (Fig. 1S) and SEM/TEM images indicated the formation mesoporousduring ZSM-5 synthesis. Possible mechanism for creation of mesoporous in ZSM-5 may be ; due to more favorable synthesis parameters such as molar gel composition, and hydrothermal crystallization at 150^0C, optimum concentration of TPABr which promote the formation of kinetically favored ZSM-5 nuclei. During crystal growth, ZSM-5 nuclei are transferred into ZSM-5 crystal and CTMABr surfactant is embedded in the ZSM-5 crystals (path 2)[21]. In calcination, Finally, surfactant and organic templates were removed which generate mesoporosity in microporous ZSM-5 crystal. Which is clearly seen in the TEM image of ,ZSM-$5_{CTA-0.06}$(Fig. 4b).Proposed mechanism is well line with mechanism proposed by R. Sabarish et al.[21], similar type of mechanisim also proposed by Yunjuan Zhang et al.[22] for preparation of hallow ZSM-5 using excess TPABr concentration.

3.3 Catalytic performance: Fructose to 5-EMF

As presented in reaction Scheme 2, synthesis of 5-EMF (biofuel additive) from fructose is occurred with two step reaction mechanism in which first step involve dehydration of fructose to 5-HMF and then etherification of 5-HMF in presence of ethanol to 5-EMF[17, 23]. In addition to acidity of catalyst, mesoporosity, which overcome steric hindrance and improve accessibility of active site, play vital role to improve catalytic performance. Characterization of ZSM-$5_{CTA-0.04,}$ ZSM-$5_{CTA-0.06}$, and ZSM-$5_{CTA-.0.1}$ indicated presence of mesoporosity which is beneficial for said reaction in comparison to conventional microporous ZSM-5.

Under identical set of reaction conditions, the performance of ZSM-5, ZSM-$5_{CTA-0.04}$, ZSM-$5_{CTA-0.06}$, and ZSM-$5_{CTA-.0.1}$ for Fructose to 5-EMF were evaluated. The results are depicted in Fig. 6, after 8 h at 125°C. All studied catalysts provide more than 95% conversion. It is noted that, in order to have complete

material balance, there must be other unidentified products, either degradation by-products (humin-type) or intermediates such as ethyl-fructoside, and ethyl glucoside etc.[24] As illustrated in Table 2, micro-ZSM-5 gave 4.6% yield of EMF and 7% of HMF, which is the lowest activity (11.6% combined yield of HMF and EMF) in spite of having acidity, 100% crystallinity and maximum microporosity. In case of micro-meso ZSM-5, 15% EMF yield, 9.2% HMF with 24.2 combined (HMF + EMF) yield was achieved over ZSM-$5_{CTA-0.04}$ at similar reaction condition. In another case, ZSM-$5_{CTA-0.06}$ showed even more improved activity with 24% EMF yield, 9.5% HMF and 33.5% combined (HMF + EMF) yield. Almost 2 and 3 fold increase in activity over ZSM-$5_{CTA-0.04}$ and ZSM-$5_{CTA-0.06}$ than ZSM-5 can be attributed to the comparatively higher mesoporous character i.e. S_{meso}(72 and 98 m2/g), V_{meso} (0.09 and and 0.10 cc/g) forZSM-$5_{CTA-0.04}$ and ZSM-$5_{CTA-0.06}$ respectively than conventional micro-ZSM-5 (S_{meso} =30 m^2/g and V_{meso}= 0.05 cc/g). The presence of mesopores in ZSM-5 apparently promotes the access of the reactant to active sites in the interior of mesoporous zeolite. Surprisingly, in spite having sufficient mesopore character (S_{meso} =63 m^2/g and V_{meso}= 0.08 cc/g), ZSM-$5_{CTA-.0.1}$ gave very low activity of 8% EMF yield, 6% HMF and 14% combined yield. Comparatively higher micropore (S_{micro}= 405 m^2/g, V_{micro}=0.196 cc/g) in ZSM-$5_{CTA-.0.1}$than ZSM-$5_{CTA-0.04\ and}$ ZSM-$5_{CTA-0.06}$ (S_{micro}= 323–340 m^2/g, V_{micro}=0.140–0.148 cc/g) may restricted the access of the reactant to active sites and resulted in the poor activity.

In view of maximizing the EMF yield, reaction temperature was optimized over optimized ZSM-$5_{CTA-0.06}$. The reaction temperature was varied from 125°C to 175°C keeping all other parameter constant. As illustrated in Fig. 6, EMF and combined EMF + HMF yield increases from 24 to 40% and 33 to 46% as temperature increase from 125 to 165°C, respectively. The dehydration of fructose to 5-HMF and later etherification of 5-HMF with ethanol is an endothermic reaction. Hence, EMF yield increased as temperature increased. However with further increases at 175°C, decrease in yield of HMF (4%), EMF (24%) was observed, which is attributed to the reaction path has further proceeded to ethyl levulinate and levulinic acid formation of humins.

At optimized temperature, ZSM-$5_{CTA-0.06}$.exhibits 5 fold increase in the EMF % yield and almost 3 fold increase in total yield of EMF and HMF than micropous ZSM-5.

4. Conclusion

In situ mesoporosity in microporous ZSM-5 was systematically created in a controlled way without destroying ZSM-5 structure. It was found that optimum synthesis parameters such as molar gel combination; hydrothermal crystallization condition of 150C; optimum concentration of dual templates such as TPABr and CTMABr; CTMABr/SiO2 molar ratio in the range of 0.04 to 0.06 are responsible for generation of mesoporosity. Moreover, use of sodium silicate and aluminium sulphate, which are cheap and stable sources of silica and alumina, respectively, are also helps to have mesoporosity in a control way, which is probably tried for first time. The synthesized micro-meso ZSM-$5_{CTA-0.06}$ has shown 5 fold increase in 5-EMF yield. 5-EMF and combined 5-EMF + 5-HMF yield increases from 24 to 40% and 33 to

46% as temperature increase from 125 to 165□C, respectively. This is probably the highest activities from fructose in one-step.

Declarations

Ethics approval and consent to participate: Not applicable

Consent for publication: Not applicable

Availability of data and materials: All data and material generated or analysed during this study are included in this published article

Funding: Not applicable

Authors' contributions: PNM did experimental work, including characterization and has written 1st draft of the manuscript. PSN and SUN did characterization, interpreted data and revised the manuscript. VVB is the principal investigator.

Acknowledgements: Not applicable

Authors' information (optional): Catalysis & Inorganic Chemistry Division, CSIR-National Chemical Laboratory,Dr.HomiBhabha Road, Pashan, Pune 411008, INDIA.

Prajakta N. Manal, Prashant S. Niphadkar, Sachin U. Nandanwar, Vijay V. Bokade

Corresponding author Vijay V. Bokade

References

1. S. Bao, G. Liu, X. Zhang, L. Wang, and Z. Mi, Ind. Eng. Chem. Res. **49**, 3972 (2010).
2. D. P. Serrano, J. Aguado, G. Morales, J. M. Rodríguez, A. Peral, M. Thommes, J. D. Epping, and B. F. Chmelka, Chem. Mater. **21**, 641 (2009).
3. D. Wang, X. Li, Z. Liu, Y. Zhang, Z. Xie, and Y. Tang, J. Colloid Interface Sci. **350**, 290 (2010).
4. N. R. Shiju and V. V. Guliants, Appl. Catal. A Gen. **356**, 1 (2009).
5. M. Bejblová, D. Procházková, and J. Čejka, ChemSusChem **2**, 486 (2009).
6. L. YOUNG, J. Catal. **76**, 418 (1982).
7. N. Chu, J. Yang, C. Li, J. Cui, Q. Zhao, X. Yin, J. Lu, and J. Wang, Microporous Mesoporous Mater. **118**, 169 (2009).
8. J.-B. Koo, N. Jiang, S. Saravanamurugan, M. Bejblová, Z. Musilová, J. Čejka, and S.-E. Park, J. Catal. **276**, 327 (2010).
9. M. Choi, K. Na, J. Kim, Y. Sakamoto, O. Terasaki, and R. Ryoo, Nature **461**, 246 (2009).

10. Y. Zhu, Z. Hua, J. Zhou, L. Wang, J. Zhao, Y. Gong, W. Wu, M. Ruan, and J. Shi, Chem. - A Eur. J. **17**, 14618 (2011).
11. L. Emdadi, D. T. Tran, E. Schulman, L. Wei, W. Shang, H. Chen, and D. Liu, Microporous Mesoporous Mater. **275**, 31 (2019).
12. J. Groen, Microporous Mesoporous Mater. **69**, 29 (2004).
13. C. R. Patil, P. S. Niphadkar, V. V. Bokade, and P. N. Joshi, Catal. Commun. **43**, 188 (2014).
14. Q. Wang, S. Xu, J. Chen, Y. Wei, J. Li, D. Fan, Z. Yu, Y. Qi, Y. He, S. Xu, C. Yuan, Y. Zhou, J. Wang, M. Zhang, B. Su, and Z. Liu, RSC Adv. **4**, 21479 (2014).
15. M. L. Gonçalves, L. D. Dimitrov, M. H. Jordão, M. Wallau, and E. A. Urquieta-González, Catal. Today **133–135**, 69 (2008).
16. P. S. Niphadkar, A. C. Garade, R. K. Jha, C. V. Rode, and P. N. Joshi, Microporous Mesoporous Mater. **136**, 115 (2010).
17. Y. Bai, L. Wei, M. Yang, H. Chen, S. Holdren, G. Zhu, D. T. Tran, C. Yao, R. Sun, Y. Pan, and D. Liu, J. Mater. Chem. A **6**, 7693 (2018).
18. N. P. Tangale, P. S. Niphadkar, P. N. Joshi, and P. L. Dhepe, Microporous Mesoporous Mater. **278**, 70 (2019).
19. K. S. W. Sing, Pure Appl. Chem. **57**, 603 (1985).
20. L. Su, L. Liu, J. Zhuang, H. Wang, Y. Li, W. Shen, Y. Xu, and X. Bao, Catal. Letters **91**, 155 (2003).
21. R. Sabarish and G. Unnikrishnan, J. Porous Mater. **27**, 691 (2020).
22. Y. Zhang and S. Che, Chem. – A Eur. J. **25**, 6196 (2019).
23. A. Pande, P. Niphadkar, K. Pandare, and V. Bokade, Energy & Fuels **32**, 3783 (2018).
24. G. Morales, M. Paniagua, J. A. Melero, and J. Iglesias, Catal. Today **279**, 305 (2017).

Schemes

Schemes 1 and 2 are available in the Supplementary Files section

Tables

Table 1: Textural and chemical properties of ZSM-5. ZSM-$5_{CTA\text{-}0.04}$,ZSM-$5_{CTA\text{-}0.06}$, and ZSM-$5_{CTA\text{-}.0.1}$

Samples	Surface area (m^2/g)			Pore Volume (cc/g)			SiO_2/Al_2O_3
	S_{BET}	S_{Meso}	S_{Micro}	V_{total}	V_{Meso}	V_{Micro}	
ZSM-5	402	30	372	0.210	0.05	0.160	100
$ZSM\text{-}5_{CTA\text{-}0.04}$	412	72	340	0.238	0.09	0.150	100
$ZSM\text{-}5_{CTA\text{-}0.06}$	421	98	323	0.240	0.10	0.140	100
$ZSM\text{-}5_{CTA\text{-}.0.1}$	468	63	405	0.276	0.08	0.196	100

Table 2 is not available with this version.

Figures

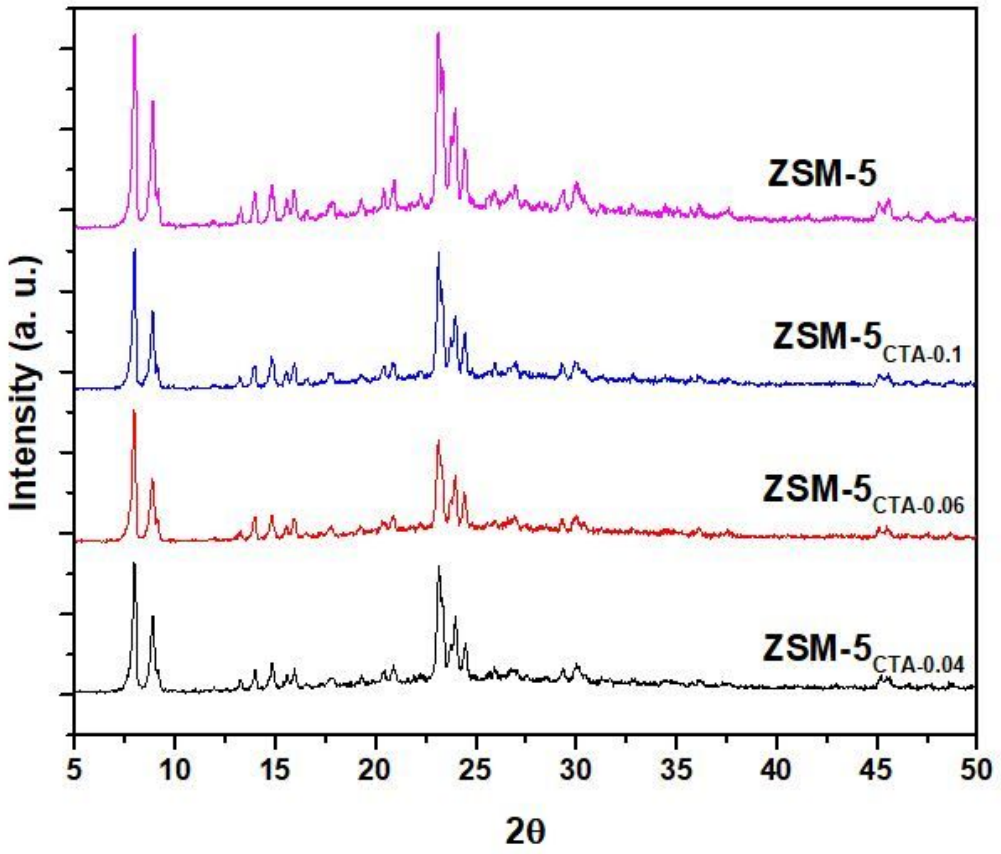

Figure 1

Powder X-ray diffraction pattern of ZSM-5 &Mesoporous ZSM-5

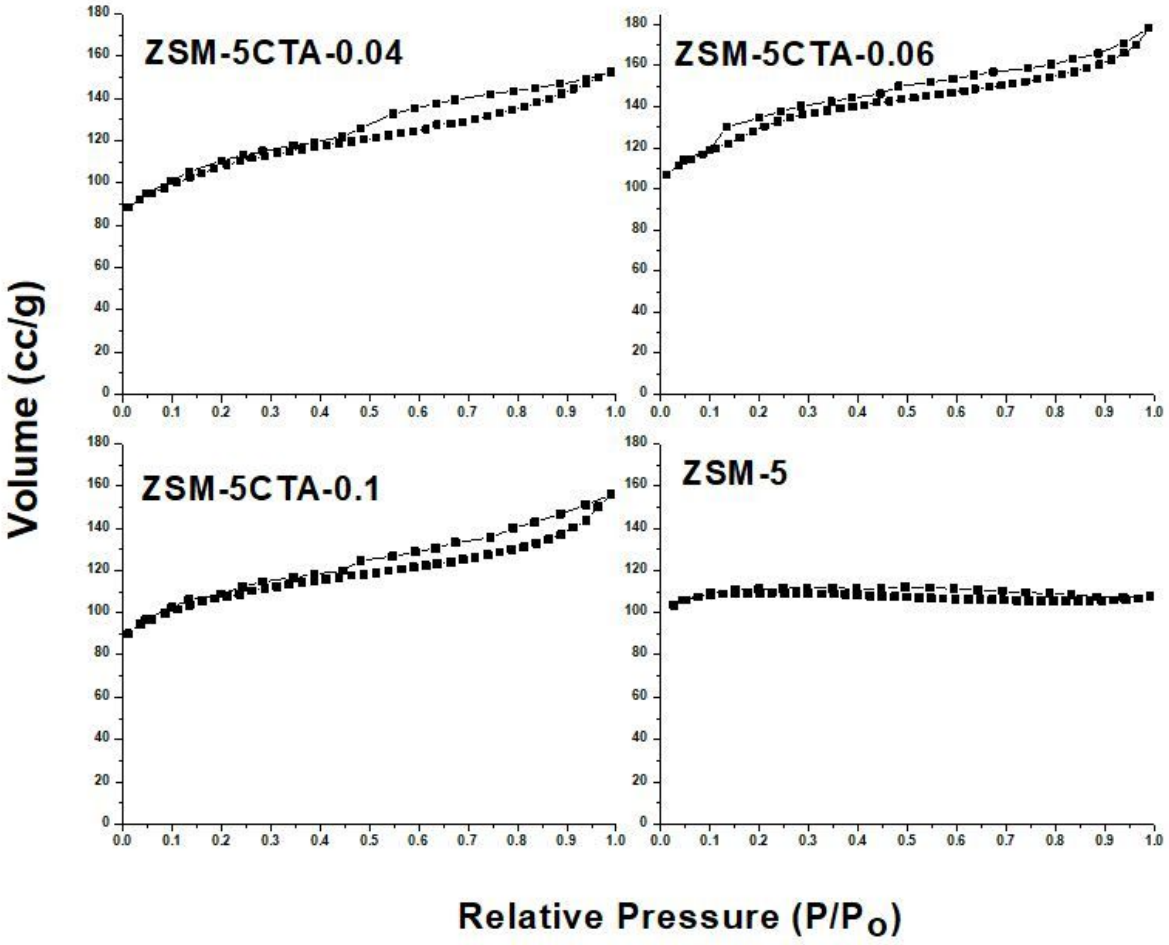

Figure 2

Isotherm of N_2 adsorption and desorption of ZSM-$5_{CTA\text{-}0.04}$,ZSM-$5_{CTA\text{-}0.06}$,ZSM-$5_{CTA\text{-}.0.1}$, and ZSM-5

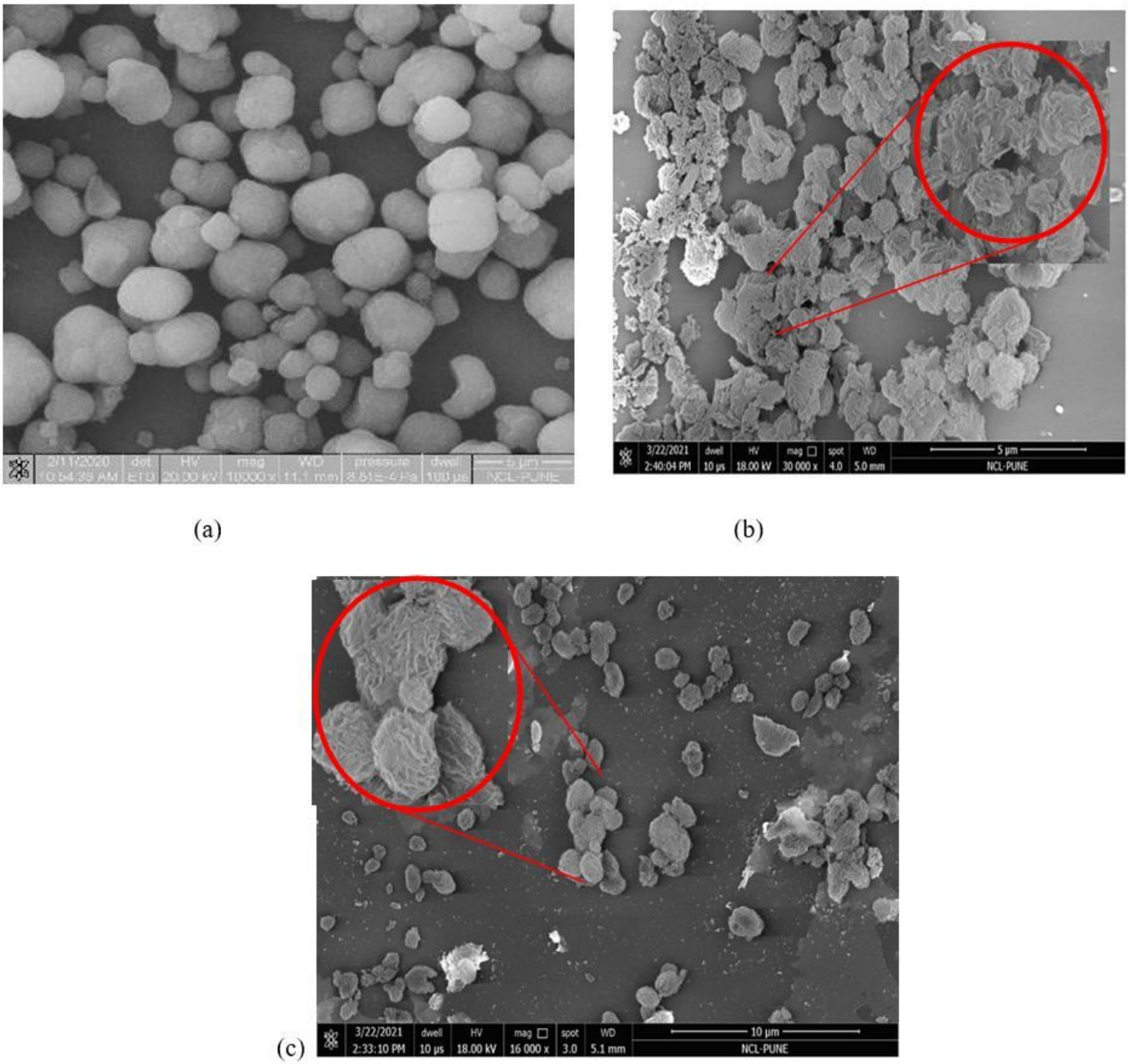

Figure 3

SEM image of (a) ZSM-5,(b) ZSM-$5_{CTA-0.04}$ and (C) ZSM-$5_{CTA-0.06}$

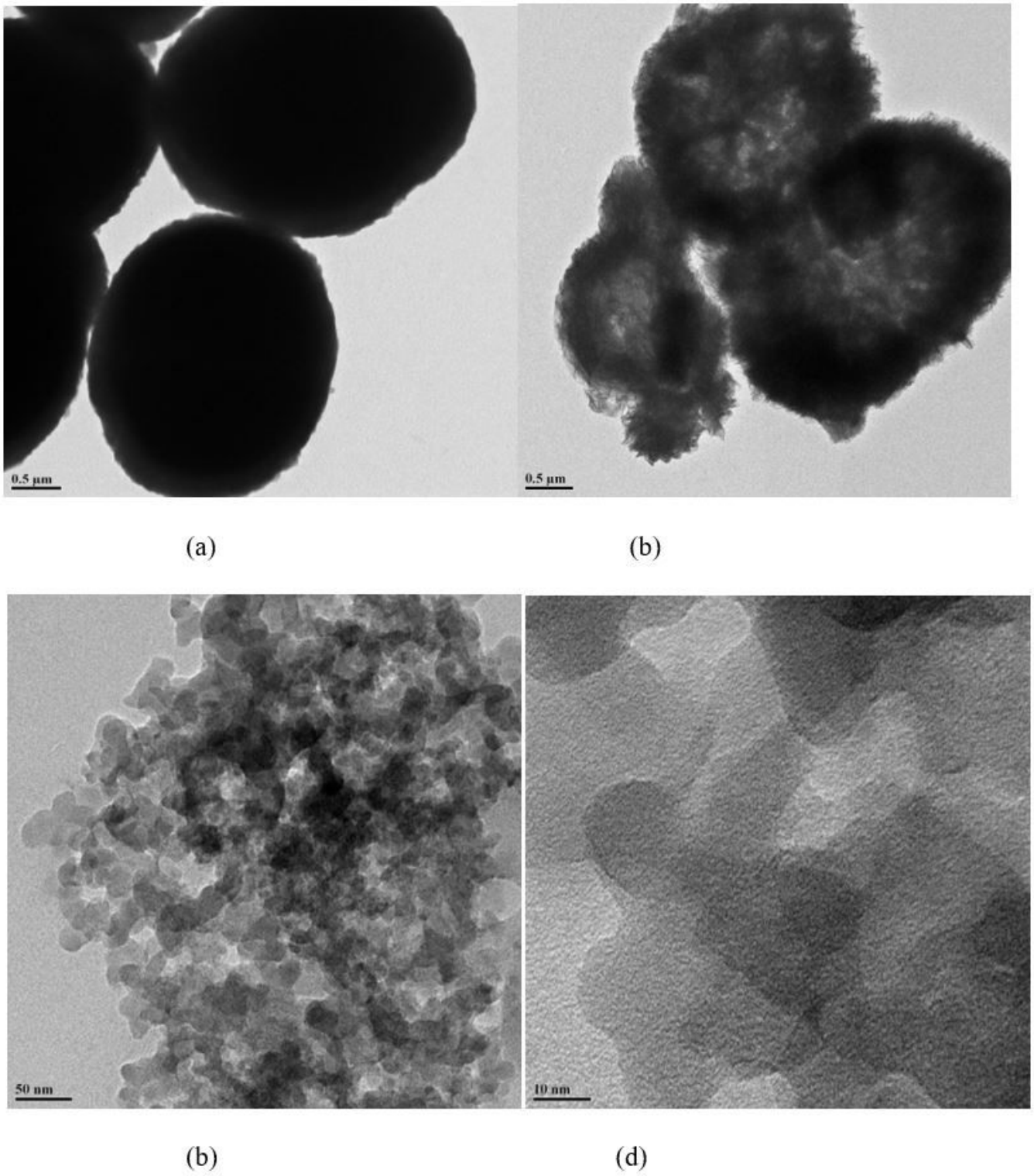

Figure 4

Representative TEM image of (a) ZSM-5,(b)ZSM-$5_{CTA-0.06}$, (c) and (d) magnified TEM image of ZSM-$5_{CTA-0.06}$

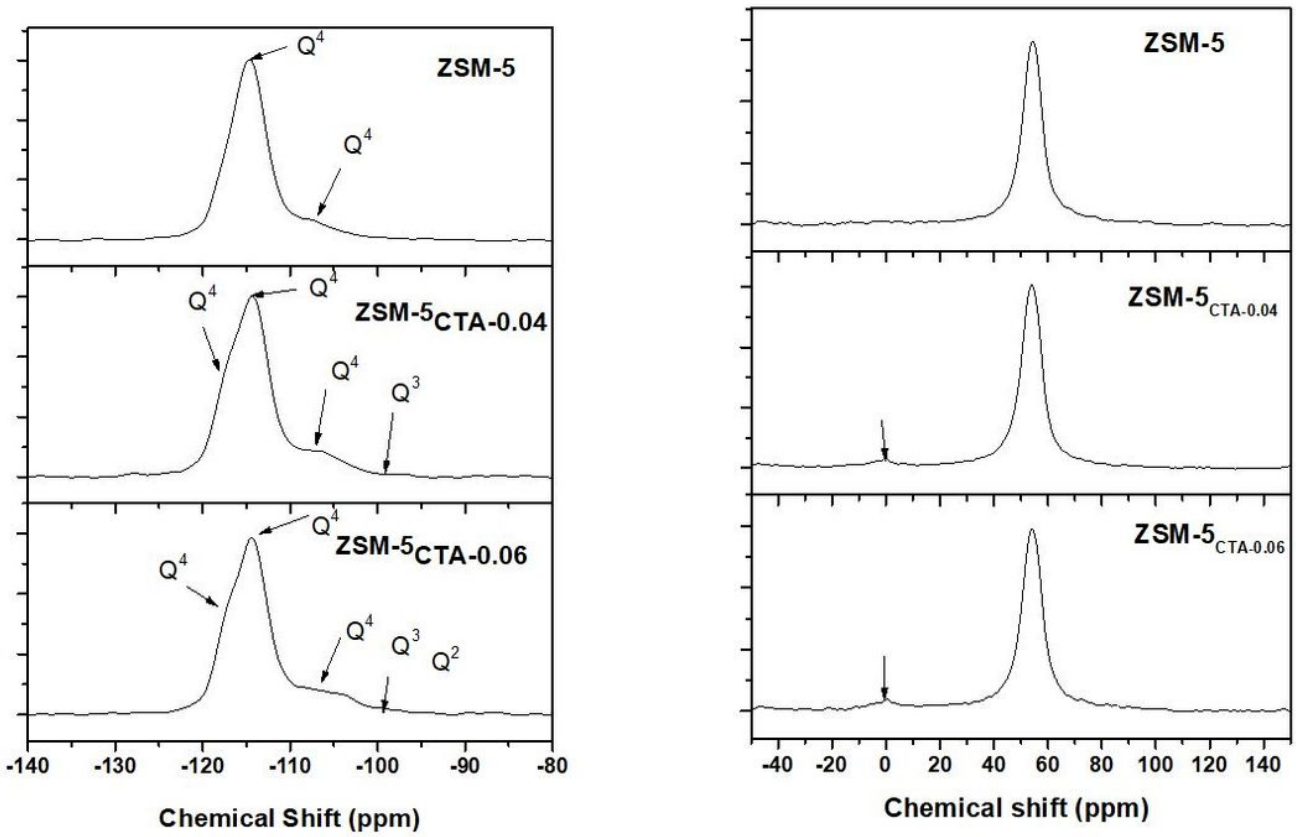

Figure 5

(a) ^{29}Si MAS NMR and (b) ^{27}Al MAS NMR spectra of ZSM-5,ZSM-5$_{CTA-0.04}$, ZSM-5$_{CTA-0.06}$.

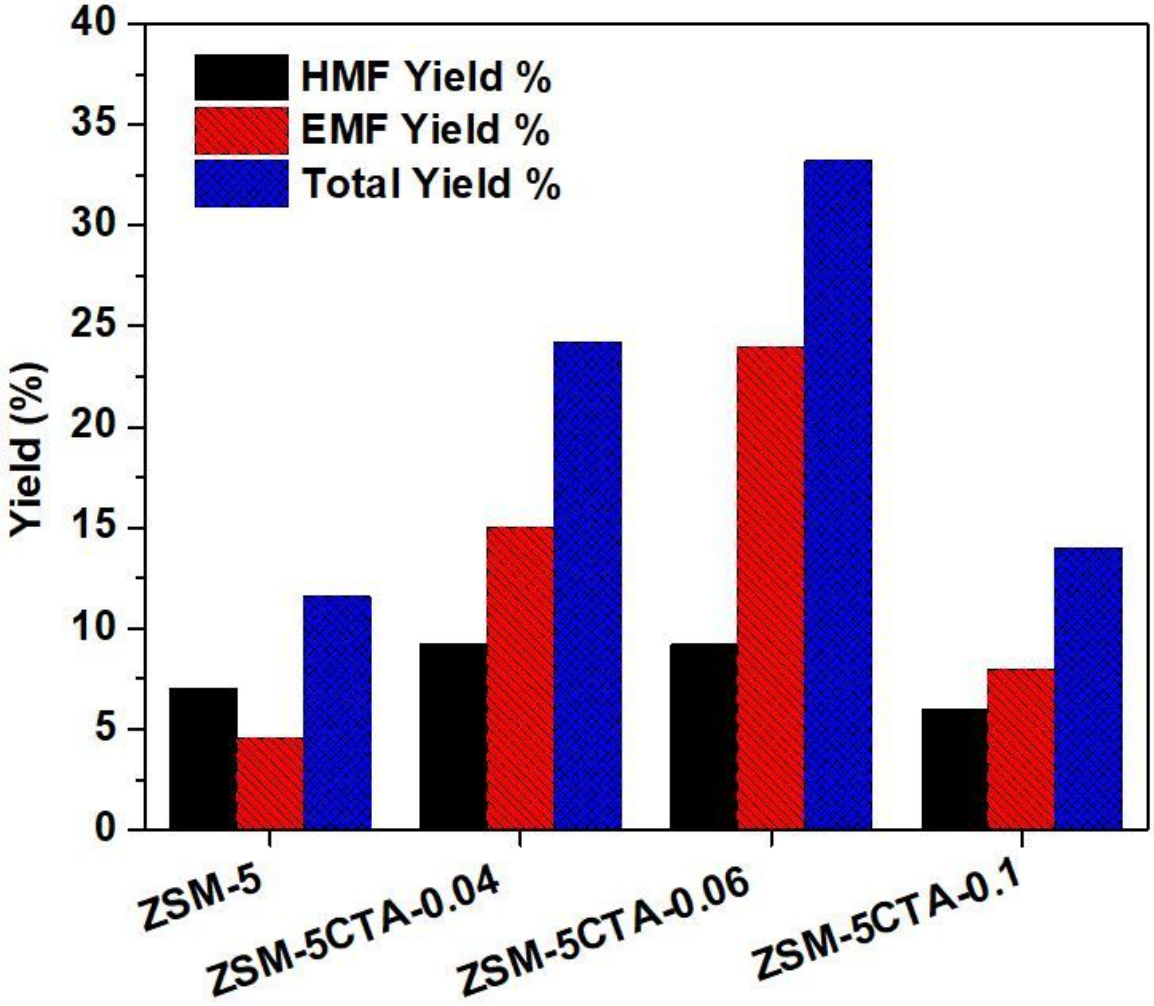

Figure 6

Fructose to EMFover ZSM-5,ZSM-$5_{CTA-0.04}$, ZSM-$5_{CTA-0.06}$, and ZSM-$5_{CTA-.0.1}$. (Reaction Condition: Fructose: 0.57g, Ethanol :15ml, Catalyst : 0.3 g Temp.: 125◦C , Time: 8h)

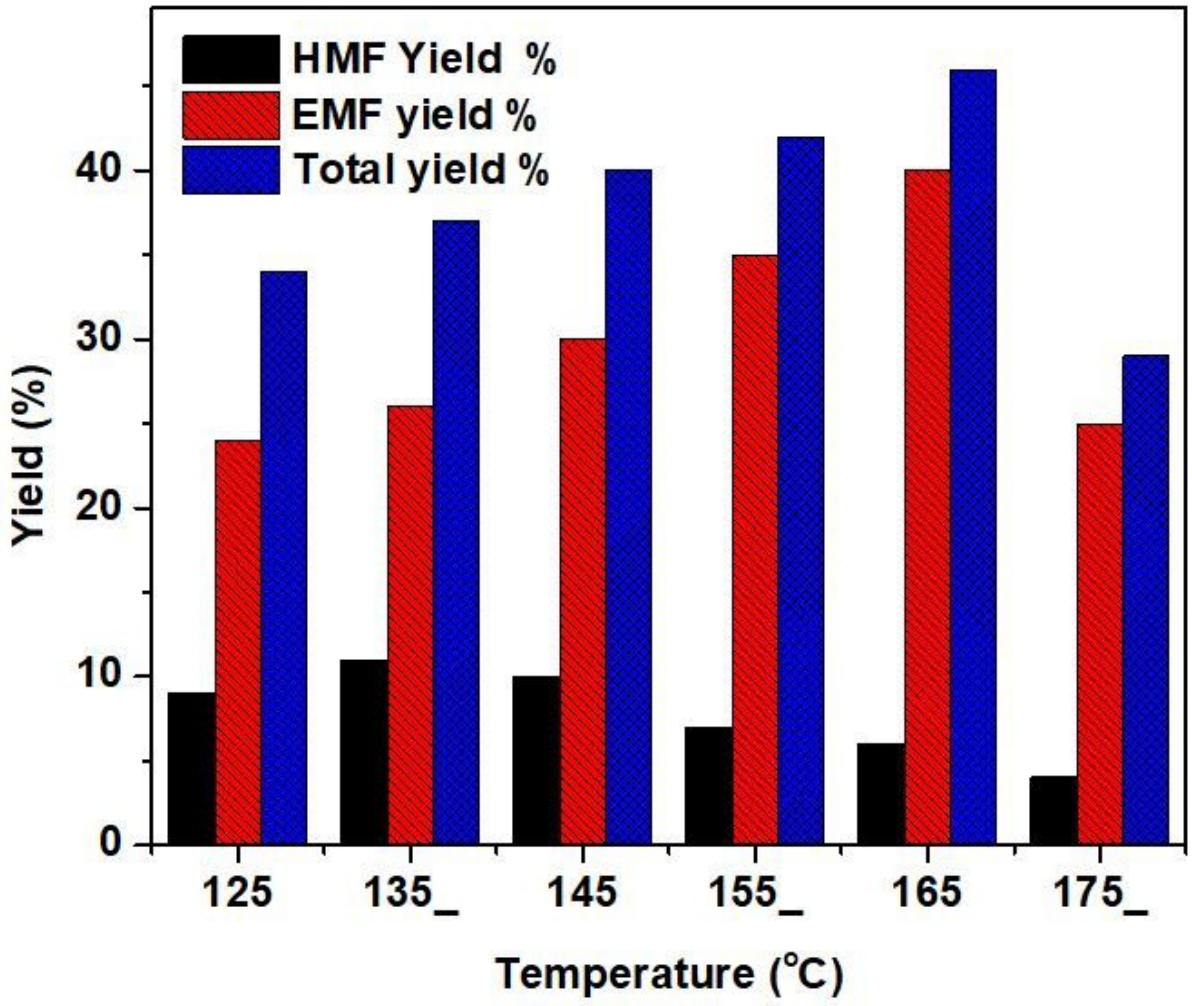

Figure 7

Effect temperature on HMF and EMF yield (Reaction Condition: Fructose: 0.57g, Ethanol : 15 ml,ZSM-$5_{CTA\text{-}0.06}$: 0.3g, Temp.: 125- 175◦C , Time: 8h)

Supplementary Files

This is a list of supplementary files associated with this preprint. Click to download.

- Scheme1.jpg
- Scheme2.jpg
- Supportinginformation.docx